A COMPUTER-BASED MODEL OF SPACE INTEGRATING ACOUSTO-OPTIC SIGNAL PROCESSING

John P. Powers, LCDR Daniel E. Smith, LCDR Michael Carmody, and LT Weldon Regan III

Department of Electrical Engineering
Naval Postgraduate School
Monterey, California 93940

Abstract

This paper presents a computer based model of general purpose signal processors that use an acousto-optic (Bragg) cell for spatially forming the spectrum of an RF signal (i.e., spatially integrating processors). The model includes the ability to represent: (1) arbitrary transfer functions for the acoustic transducer, (2) arbitrary beam profile for the incident laser beam, (3) diffraction effects as the light forms the spectrum, and (4) diffraction inefficiency due to a multi-frequency acoustic signal. The model has been used to predict expected sidelobe levels for various input laser beam profiles and can be used to predict tradeoffs between spot size (and hence frequency resolutions) vs. sidelobe levels. Additionally the model has been useful in an investigation of the sensitivity of optical excision processors to the placement of the excisor. It has also been used pedagogically to demonstrate many of the transient effects expected with acousto-optic processing of short RF pulses.

A schematic of a space-integrating acousto-optic signal processor is shown in Fig. 1. To a first degree of approximation the output at the detector array plane spatially represents the frequency content of the time varying Fourier components of the wideband RF signal applied to the Bragg cell [1-3]. Figure 2 compares the output of our acousto-optic testbed (center frequency of 70 MHz with a 40 MHz bandwidth) to the output of an electronic spectrum analyzer. Such systems are in use for spectrum analysis and other signal processing of RF signals up to 1 GHz in bandwidth. The degree to which the output light intensity approaches the power spectral density depends on many factors including the laser beam amplitude profile across the Bragg cell aperture, the frequency dependent acoustic

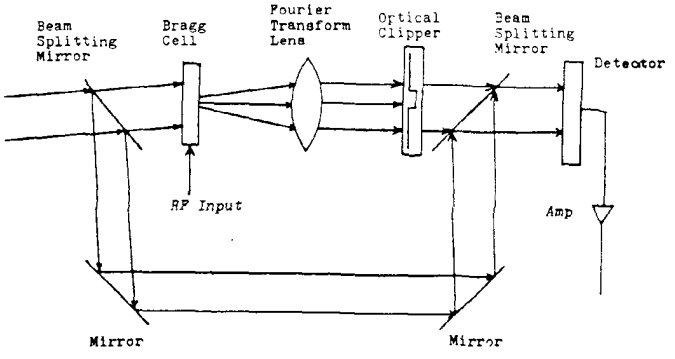

Figure 1. Schematic of an acousto-optic spectrum analyzer.

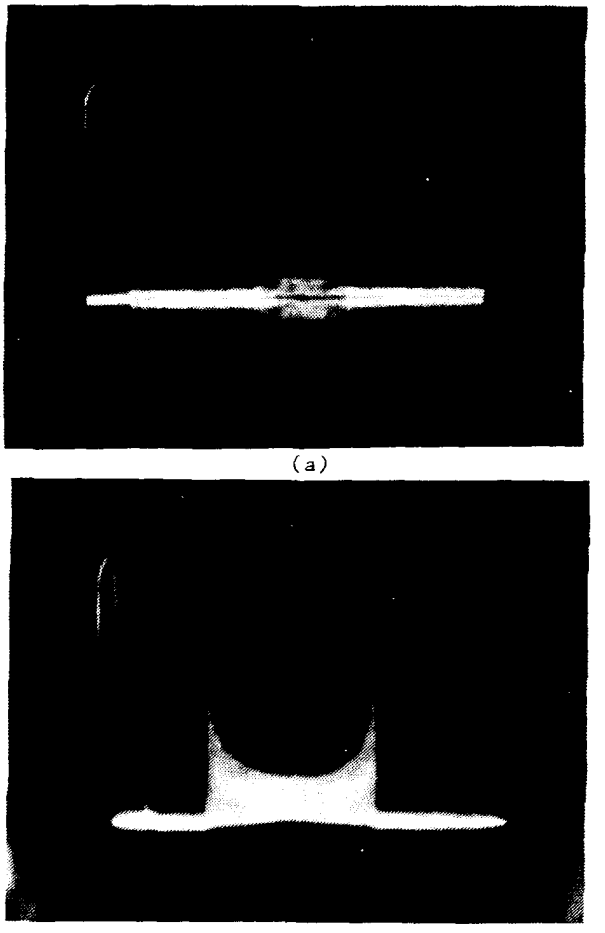

(a)

Figure 2. (a) Output of an experimental acousto-optic spectrum analyzer for an FM signal (b) Output of a conventional spectrum analyzer for the same FM signal.

attenuation, the nonuniform transfer function of the ultrasonic transducer and diffraction efficiency variation with frequency. The objective of this study was to produce an interactive computer-based model of the Bragg cell processor to investigate the effects of these factors, to allow sensitivity investigation of the system parameters, and to perform analysis of optical excision of narrowband interference [4].

The basic theory of signal analysis by acousto-optic diffraction of laser light has been described by Korpel [1] among others. Due to the frequency dispersive nature of Bragg diffraction and the angle-to-position conversion role played by the transform lens the output light amplitude E_s at position x_1 (Fig. 3) is proportional to the Fourier transform of RF signal that is in the

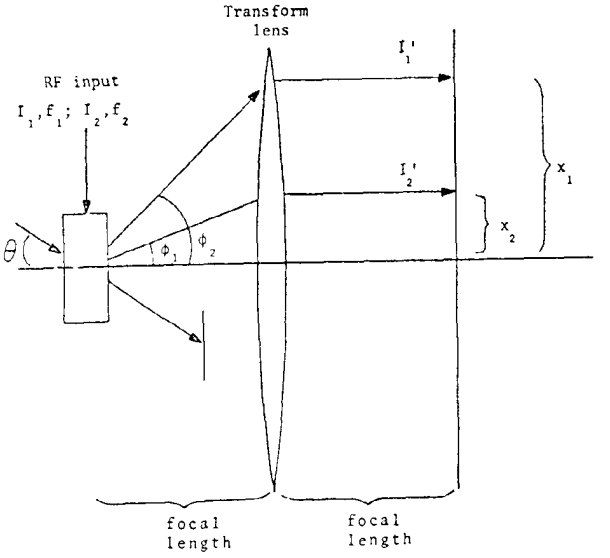

Figure 3. Geometrical parameters for Bragg cell and transform lens.

acoustic aperture, i.e.,

$$E(x_1) \alpha S(f)\ e^{j(\omega+2\pi ft)} \quad (1)$$

$$\text{where} \quad S(f) \alpha \int_{-\frac{\tau_s}{2}}^{\frac{\tau_s}{2}} s(t)\ e^{-j2\pi ft}dt \quad (2)$$

$$x_1 = \frac{\ell\lambda_o}{V_s} f \quad (3)$$

τ_s is transit time of the acoustic signal $S(t)$,

x_1 is the position on the detector plane,

ℓ is the focal length of the transform lens and,

V_s is the velocity of sound in the acoustic medium.

Equation (1) also includes a doppler-like frequency shift in the diffracted component.

Hecht [2] includes the aperture function, illuminating laser beam profile and acoustic attenuation in a weighting function $W(t - t')$ that multiplies the RF signal

$$E(f,t) \alpha \int_{-\infty}^{\infty} W(t - t')\ S(t')\ e^{-j2\pi ft'}dt' \quad (4)$$

where $E(f,t)$ is the time varying frequency component (at some position x_1 corresponding to f by Eqn. 3) as the RF signal progresses through the Bragg cell.

In our implementation we have retained this weighting function to account for arbitrary illumination beam profiles (including truncated Gaussian and plane waves, pure Gaussian beams, and apodized beams designed to achieve a variety of sidelobe requirements) and frequency dependent acoustic attenuation (which can be particularly important in large time-bandwidth systems). The finite temporal length of the acoustic signal is included in the limits of the integral when taking the FFT.

The effect of the nonideal transfer function of the RF-to-ultrasound transducer can be included by realizing that $S(t')$ in Eqn. 4 can be interpreted as the sound field after transduction. The fidelity of this sound field in duplicating the RF signal depends on the uniformity of the transfer function, a difficult goal to achieve in a wideband transducer. Since transducer models can be extremely complex [5] the program allows entry of experimentally measured frequency charactertistics which will be multiplied by the transform of the RF signal and inversely transformed to find the $S(t')$ signal inside the acoustic medium. Otherwise an ideal transfer function is assumed.

The most difficult portion of the system to model is the Bragg interaction between the light and the sound. While the interaction geometry between the light and the sound can be optimized for one frequency component (usually the center frequency), other frequency components will not be optimally aligned, suffering a reduced interaction efficiency. Attempts to alleviate this inefficiency have led to the design of phased array transducers [6, 7] (Fig. 4). The interaction between an arbitrary-shaped coherent light beam and a wideband arbitrarily shaped acoustic field under the strong interaction conditions usually found in a Bragg Cell is quite difficult to model. The weak interaction of an arbitrary light beam with a single frequency rectangular sound column has been modelled by Chu and Kong [8]. Extension to a wideband sound

source by temporal Fourier decomposition should give a close approximation to the interaction within the Bragg cell and the resulting light pattern. Korpel [9] has produced a model for strong interaction between arbitrary light beams and single frequency sound beams using plane-wave decomposition of the beams and multiple scattering

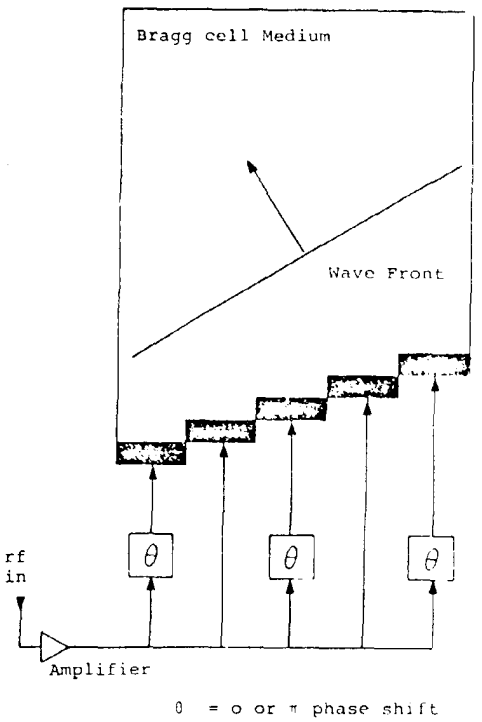

Figure 4. Schematic of a phased array transducer.

theory. Based on plane wave-plane wave interactions and Chang's [10] work with coupled equations, Hecht [5] has written an expression for the frequency dependent portion of the diffraction efficiency for a single element transducer with a wideband signal as:

$$\frac{I_1}{I_o} \alpha \frac{\sin^2[\pi/2L/L_o\{FF_m - F^2\}]}{\pi/2L/L_o\{FF_m - F^2\}} \qquad (5)$$

where

I_1 and I_o are the diffracted and undiffracted beam intensities,

F is the normalized center frequency = 1,

F_m is the input frequency normalized to the center frequency value,

L is the interaction width and,

$L_o = n\Lambda_o^2 \cos\theta_o/\lambda_o$ is the characteristic interaction length with n being the refractive index of the medium, Λ_o is the acoustic wavelength at the center frequency, θ_o is the Bragg angle at the center frequency and λ_o is the free space light wavelength.

Figure 5 shows a plot of Eqn. 5 for various ratios of L/L_o indicating severe variation with frequency for large values of L/L_o. Pinnow [6] gives design rules and expressions for the diffraction efficiencies of phased array transducer.

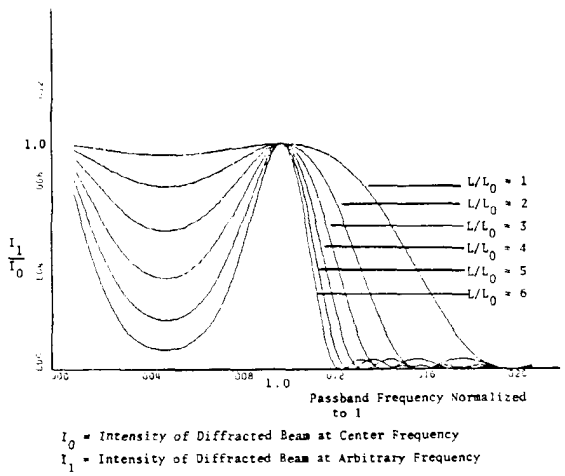

Figure 5. Diffraction efficiency bandshape for a single element transducer (after [2]).

In our model diffraction inefficiency is handled in one of two ways. Since calibration curves are easily measured that indicate the relative light output for a constant-amplitude variable frequency calibration RF signal, provision is made for the entry of this data. Since this calibration data includes the transducer's conversion efficiency as well, the user should assume a uniform transducer transfer function in that part of the program. Use of this mode however inhibits the application of the model as a design aid in optimizing the system performance. Lacking the calibration measurements the efficiencies of Eqn. 5 are used for single element transducers as an approximation to the correct inefficiency. Future work would include adding models for phased array transducer. This portion of our model needs future upgrading to include more rigorous theories that model the interaction in the Bragg cell.

The resulting computer program that is our model is a Fortran program designed for running in an interactive mode on an IBM 3033 mainframe computer. Hard copy is provided on a nonreal-time basis from the plotter output. One can obtain a static presentation of the output at an instant of time (or for a continuous signal) as shown in Fig. 6 or a time series presentation of the output for short duration pulses as in Figs. 9 and 10. A run to produce a display of the static output takes approximately one second; a run producing a time series output requires several seconds of run time because of the numerous FFT's that are needed.

We have begun to apply the computer-based model in two areas of study: analysis and optimization of system parameters [11] and optical excision of narrowband interference components from wideband signals [4, 12]. In both cases use of the program allows the investigator to interactively vary component parameters or geometry to investigate the effects on the system output and to study the sensitivity of the system to various parameters. Because of the multidimensional nature of these problems combining time, frequency, three dimensions of space, amplitude and phase in a frequently interchangeable fashion and because of the myriad of electronic acoustical and optical parameters involved we feel that such a model is the only systematic way to assess system performance. A laboratory experimental system allows corroboration of the results where appropriate.

Figure 6, for example, illustrates the expected results when a Gaussian beam profile and a plane wave profile are used holding other parameters constant. (The frequency values chosen are indicative of the frequency span of the experimental system.) Extensive investigation has also been made on determining the tradeoff between sidelobe level and Gaussian beam spot size (along with the attendant variation in aperture illumination length). Figures 7 and 8 illustrate the different outputs expected from a single element transducer ($L/L_o = 2$) and that of a phased arrray. The data for the phased array efficiency was obtained from the calibration curves accompanying our Bragg cell which showed only a slight roll off in efficiency at the 50 MHz and 90 MHz ends of the passband. A wideband signal was simulated by simultaneously applying equal amplitude signals at frequencies located 5 MHz apart over the region from 50 MHz to 90 MHz. The light wave was assumed to be planar.

Figures 9 and 10 illustrate the capability of the model to represent the time varying output of the system as a narrow (1 μsec) pulse (tone burst) proceeds through the Bragg cell with a transit time of 10 μsec illustrating the nature of the pulse stretching problem common to acousto-optic processors. Figure 10 shows the time series development of the spectrum of a more complicated one microsecond burst: one undergoing a sinusoidally modulated FM signal with a modulation rate of 5MHz and a frequency shift of 40 MHz about a center frequency of 70 MHz. Both figures assume a Gaussian beam input and a stepped array transducer although other cases have been simulated as well [11].

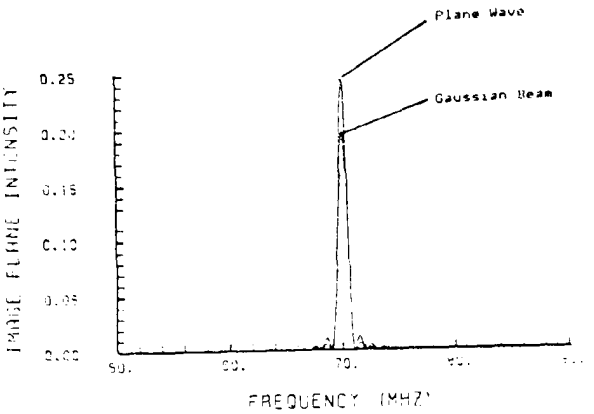

Figure 6. Comparative transform plane intensity profiles for Gaussian and planar incident beams.

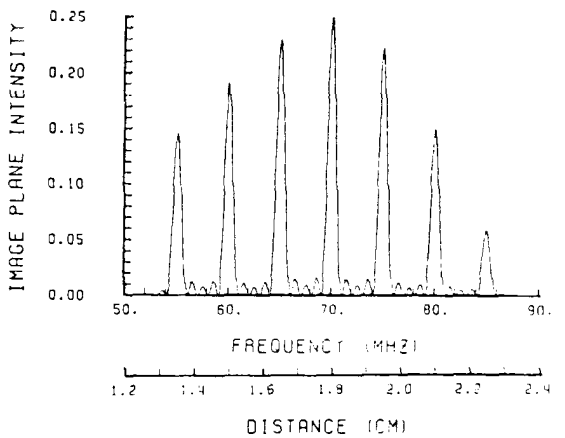

Figure 7. Transform plane intensity profile for wideband comb signal for a single element transducer ($L/L_o = 2$).

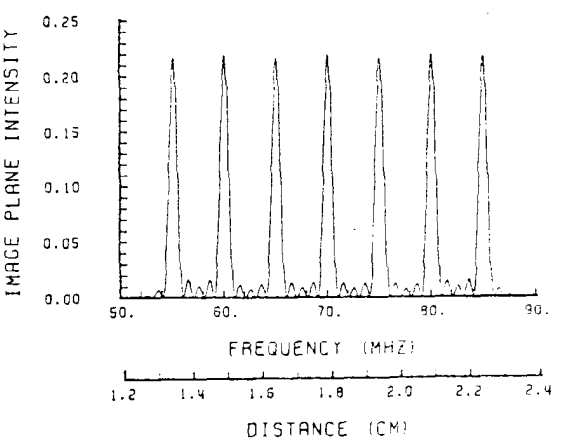

Figure 8. Transform plane intensity profile for wideband comb signal and a phased array transducer.

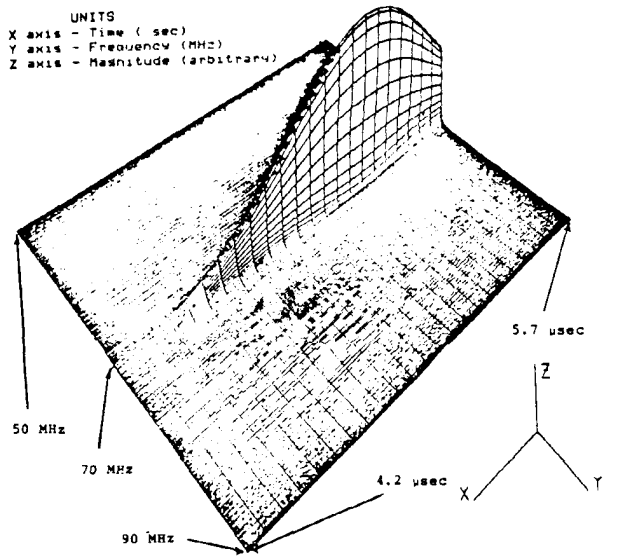

Figure 9. Representative time series intensity output for 1 μsec tone burst of 70 MHz signal.

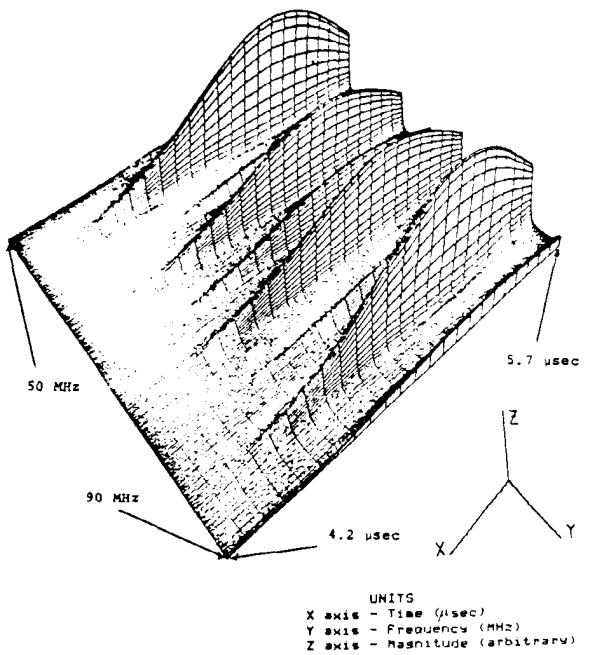

Figure 10. Representative time series intensity output for FM tone burst (see text for signal description).

The second study topic that has utilized this computer model is that of optical excision of narrowband interference from wideband signals [3] illustrated in Fig. 11. Since the optical processor presents the spectral composition of the RF signal in the transform plane, narrowband interference signals can be removed by spatial filters at that location. The spatial filters might be fixed absorption masks or electrically controlled optical spatial light modulators (if the desired mix of dynamic range, resolution and speed can be achieved). By recombining the filtered spectrum with a reference beam and heterodyne detecting the output with a large area detector (with speed adequate for detecting the highest frequency component in the original RF signal), the filtered output signal (less the interference) will be produced at the detector output. While the location of the detector in immaterial to reconstructing signal, assuming that it intercepts all of optical spectrum, the sensitivity of the location of the optical filter was of interest as were the effects of optical diffraction around the obstacle [4, 12]. Figure 12 illustrates the desired signal and the interference with a potential solution by placing the obstacle as shown. Figure 13 shows the result of using the computer based model as modified to attack this problem. (The position of the obstacle and desired signal are reversed from the previous figure.) By calculating the ratios of the signal power to interference power both before and after processing, one can use this S/I ratio as a figure of merit to optimize the obstacle size for a given spacing between the signal and the interference and hence obtain the optimum S/I ratio as shown in Table I. Further studies have also been done for obstacles with tapered attenuation and for various laser beam profiles.

The model has proven most useful in simulation studies of acousto-optic processing systems. Further extensions to the model, beside expanding the light-sound interaction representation include laser amplitude noise effects and most importantly, detector effects. Currently the model assumes ideal detector response in dynamic range and frequency. Since these areas are currently major bottlenecks in acousto-optic processing systems a realistic model of this component would be most useful.

The authors would like to acknowledge the partial support of the Naval Electronics System Command (ELEX 350) for this work.

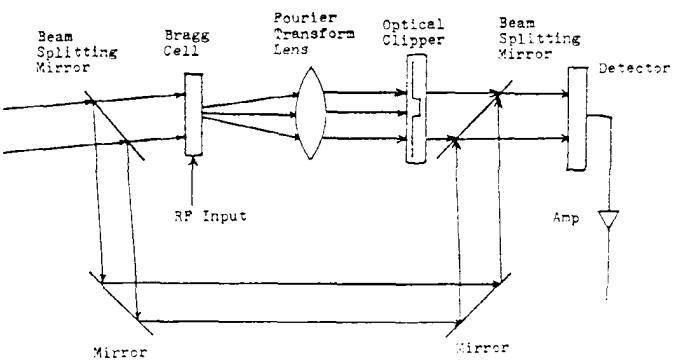

Figure 11. Schematic for acousto-optic spectrum excision with heterodyne detection.

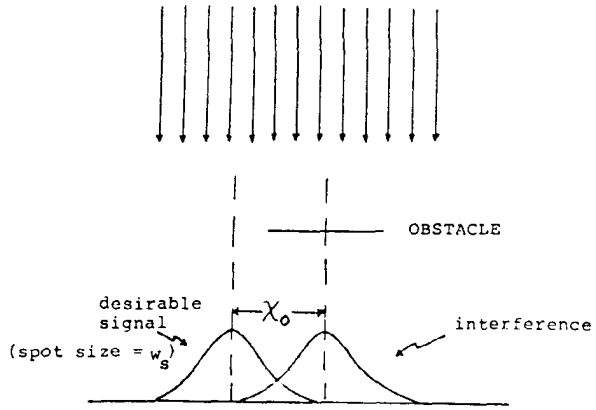

Figure 12. Geometry for optical excision of narrowband interference by an obstacle.

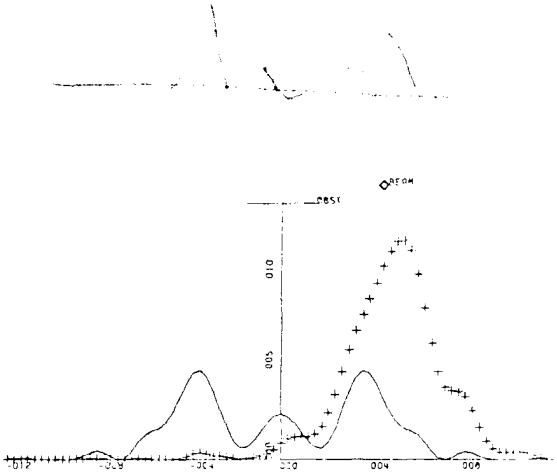

Figure 13. Representative results of optical excision by an obstacle (reversed from previous figure). Solid curve = interference, curve + signs = signal beam.

Offset	Optimum Obstacle Size	Optimum S/I Ratio	Optimum S/I Ratio (dB)
0.05	2.4	1.14	0.57
0.10	2.45	1.55	1.90
0.15	2.55	2.32	3.65
0.20	2.55	3.82	5.82
0.25	2.65	6.62	8.21
0.30	2.70	~10	~10
0.35	2.65	~18	~12.5

Table I. Representative computer calculated optimum obstacle widths and signal/interference ratios for small offset distances between signal and interference beams.

References

1. Korpel, A., "Acousto-optics," Applied Solid State Science, v. 3, R. Wolfe, Ed., pp. 71-180, Academic Press, 1972.

2. Hecht, D. L., "Spectrum Analysis Using Acousto-optic Devices," Optical Engineering, pp. 461-466, September/October 1977.

3. Turpin, T. M., "Spectrum Analysis Using Optical Processing," Proc. IEEE, v. 69(1), pp. 79-92, January 1981.

4. Smith, D. E., "Acousto-optic Spectral Excision of Narrowband Interference," Engineer's Thesis, Naval Postgraduate School, Monterey, CA, 1980 (Unpublished).

5. Young, E. H., and Yao, S-K., "Design Considerations for Acousto-optic Devices," Proc. IEEE, v. 69(1), pp. 54-64, January 1981.

6. Pinnow, D. A., "Acousto-optic Light Deflection: Design Considerations for First Order Beam Steering Transducers," IEEE Trans. on Sonics and Ultrasonics, v. SU-18, pp. 209-214, October 1971.

7. Tsai, C. S., "Guided-Wave Acousto-optic Bragg Modulators for Wideband Integrated Optic Communications and Signal Processing," IEEE Trans. on Circuits and Systems, v. CAS-26(12), pp. 1072-1098, December 1979.

8. Chu, R. S., and Kong, J. A., "Diffraction of Optical Beams with Arbitrary Profiles by a Periodically Modulated Layer," J. of Opt. Soc. Am., v. 70(1), pp. 1-6, January 1980.

9. Korpel, A., "Two-dimensional Plane Wave Theory of Strong Acousto-optic Interaction in Isotropic Media," J. of Opt. Soc. Am., v. 69(5), pp. 678-683, May 1979.

10. Chang, I. C., "Acoustooptic Devices and Applications," IEEE Trans. on Sonics and Ultrasonics, v. SU-23, pp. 2-23, January 1976.

11. Carmody, M. J., "Acoustooptical Spectrum Analysis Modeling," Master's Thesis, Naval Postgraduate School, Monterey, CA, 1981 (Unpublished).

12. Regan, F. W., "Acoustooptic Spectrum Analysis and Narrowband Interference Excision in Wideband Signal Environments," Electrical Engineer's Thesis, Naval Postgraduate School, Monterey, CA, 1979, (National Technical Information Service Report Number AD-A078 286/2).